JOURNAL OF NEUROTRAUMA
Volume 20, Number 4, 2003

Influence of Impact Direction on the Human Head in Prediction of Subdural Hematoma

SVEIN KLEIVEN

ABSTRACT

The objective of the present study was to analyze the effect of different loading directions following impact, and to evaluate existing global head injury criteria. Detailed and parameterized models of the adult human head were created by using the Finite Element Method (FEM). Loads corresponding to the same impact power were imposed in different directions. Furthermore, the Head Injury Criterion (HIC) and the recently proposed Head Impact Power (HIP) criterion were evaluated with respect to the relative motion between the skull and the brain, as well as the strain in the bridging veins. It was found that the influence of impact direction had a substantial effect on the intracranial response. The largest relative skull-brain motion and strain in the bridging veins occurred with the anterior-posterior (AP) and posterior-anterior (PA) rotational impulses. HIC was unable to predict consequences of a pure rotational impulse while HIP needed individual scaling coefficients for the different terms to account for difference in load direction. When using the proposed scaling procedure, a better prediction of subdural hematoma (SDH) was obtained. It is thus suggested that an evaluation of the synergistic terms is necessary to further improve the injury prediction. These variations should be considered when developing new head injury criteria.

Key words: finite element method (FEM); head impact power (HIP); head injury; head injury criterion (HIC)

INTRODUCTION

In Europe, road accidents are the second most frequent cause of death preceded only by cancer (European Transport Safety Council, 1999). For people younger than 45 years, the frequency of death or severe injury from road accidents is about six times higher than that from cancer. A significant number of road accidents affect the central nervous system (CNS) in a devastating way by transferring high kinetic energy to the nervous tissue. Subdural hematomas (SDH) and diffuse axonal injuries (DAI) are more lethal than most other brain lesions (Gennarelli and Thibault, 1982). This gives a special interest in deriving injury criteria for SDH and DAI. Gennarelli (1983) suggested that SDH was produced by short duration and high amplitude of angular accelerations, while DAI was produced by longer duration and low amplitude of coronal accelerations. A threshold for DAI has been proposed (Margulies and Thibault, 1992) which accounts for rotational impulses in the coronal plane. Using collision tests with cadavers, Löwenhielm (1974a) hypothesised that bridging vein disruption due to an AP rotational movement of the head is obtained when the angular acceleration exceeds 4.5 krad/sec^2 and/or the change in angular velocity exceeds 50 rad/sec. On the other hand, the motions were not purely rotational,

Department of Aeronautics, Royal Institute of Technology, Stockholm, Sweden.

and either none or several bridging veins were ruptured, indicating that a real threshold was not found. Moreover, studies by DiMasi et al. (1995), and Ueno and Melvin (1995) found that the use of either translation or rotation alone may underestimate the severity of an injury. Generally, the head injury criterion (HIC) (National Highway Traffic Safety Adm., 1972) is used when evaluating the consequences of an impact to the head. HIC is based exclusively on the resultant translational acceleration of the head. Thus, HIC and proposed acceleration thresholds neither take into consideration rotational and translational loads, nor directional dependency. There is therefore a need for more complex injury assessment functions, accounting for both translational and angular acceleration components as well as changes in the direction of the loading.

When a comparison between translation and rotation has been performed, the usual approach has been to compare a non-centroidal rotational impulse with a translational impulse giving a similar acceleration measured at the center of gravity (c.g.) (Margulies et al., 1985; Bandak and Eppinger, 1994). This gives a good basis for criticism of head injury criteria based solely on the translational acceleration (i.e. HIC). In this case, however, the comparison will be between a translational impulse and an equal translational impulse in addition to the induced rotational one. A more objective approach would be to apply the same dosage of mechanical energy per time unit (i.e., the power) for the separate degrees of freedom as described here, as a basis for a new head injury criterion: HIP (Newman et al., 2000).

The influence of certain impact directions have been investigated for DAI (Gennarelli et al., 1982, 1987) and cerebral concussion (Hodgson et al., 1983). In both studies, non-human primates were used. In a three-dimensional (3D) numerical study (Zhang et al., 2001), brain responses between frontal and lateral impacts were compared. This study confirmed earlier results by Gennarelli et al. (1982) that loads in the lateral direction are more likely to cause DAI than impulses in the sagittal plane. However, a tied interface was imposed between the skull and the brain leaving out any possibility of evaluating relative motion-induced injuries such as SDH. Zhou et al. (1995) suggested that SDH is more easily produced in an occipital impact than in a corresponding frontal one. Later, the same researchers (1996) found that AP motion causes higher strain in the bridging veins than a corresponding lateral motion. Nevertheless, both studies utilized a tied interface between the skull and the brain, which is unlikely to allow any large relative motion between the skull and the brain. Since the strain observed in the bridging veins is highly dependent on the amount of relative motion between the skull and the brain, this questions the validity of these results.

Due to the limited studies of impact directions, the existing head injury criteria could not be evaluated for all types of impacts. Recently, a new global kinematic-based head injury criterion, called the HIP was presented (Newman et al., 2000). In that study, it was proposed that coefficients for the different directions could be chosen to normalize the HIP with respect to some selected failure levels for a specific direction. However, values of the coefficients were not presented and information regarding directional sensitivity was lacking.

Thus, the aim of the present investigation was to study the influence of inertial forces on all the degrees of freedom of the human head, evaluated with a detailed FE model. The HIC, as well as the HIP, were investigated with regard to their ability to take into account consequences of different impact directions for the prediction of SDH. Furthermore, scaling coefficients for the HIP are proposed for prediction of SDH.

MATERIALS AND METHODS

Finite Element Mesh

A detailed and parameterized finite element (FE) model of the adult human head was created, comprising the scalp, skull, brain, meninges, cerebrospinal fluid (CSF), and 11 pairs of parasagittal bridging veins (Fig. 1). A simplified neck, including an extension of the brain stem into the spinal cord, the dura and pia mater, the vertebrae and muscles, was also modeled.

This model has been experimentally validated against pressure data in a previous study (Kleiven and von Holst, 2002a) as well as relative motion magnitude data (Kleiven and von Holst, 2002b). Also, a comprehensive correlation between the FE model output and the relative motion between human cadaver brain and skull in anatomical X, Y, and Z components has been demonstrated for three impact directions (Kleiven and Hardy, 2002). The model has been validated with experiments performed using acceleration impulses of magnitudes and durations close to the ones in the present study.

Ventricles, Gray, and White Matter

In order to better simulate the stress and strain distribution, separate representations of gray and white matter and inclusion of the ventricles were implemented. The volume fraction of white matter to gray matter was 0.5, which is on the lower side of reported values (Blatter, 1995). The volume of the ventricles was 18 mL for the 50th percentile male geometry, which is within the reported range (Blatter, 1995).

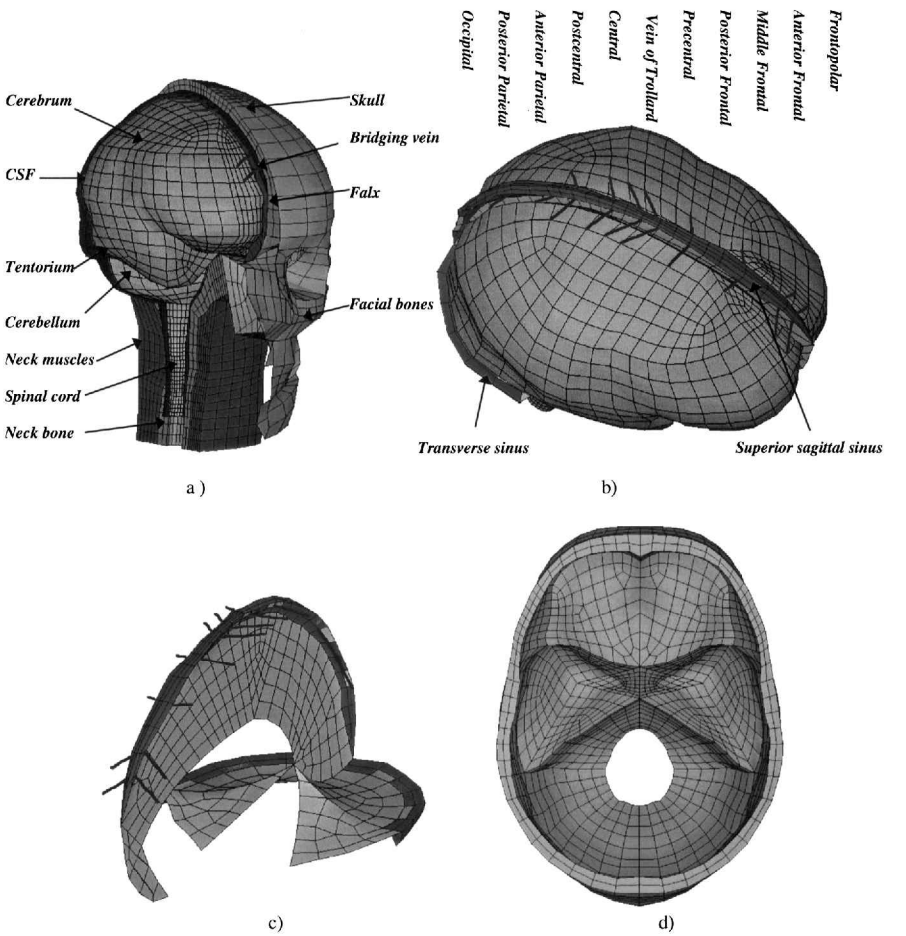

FIG. 1. Finite element mesh of (**a**) the human head; (**b**) brain, falx, and tentorium, including transverse and superior sagittal sinuses with bridging veins; (**c**) falx and tentorium; and (**d**) skull bone.

Bridging Veins

The most common type of SDH results from tearing of veins traversing the subdural space from the surface of the brain to the superior sagittal sinus (Gennarelli and Thibault, 1982). Eleven pairs of the largest parasagittal bridging veins were therefore modeled with truss elements that can only sustain load in tension. The parasagittal bridging veins drain into the superior sagittal sinus. Usually, a free segment of 10–20 mm in length is found between exit of the veins from the subarachnoidal space to their entrance into the sinus. The frontopolar and the anterior frontal veins are directed backward, to enter the sinus, at an average angle of 110o measured counterclockwise from the midsagittal line (Fig. 1b). The major parasagittal bridging veins located posterior to the frontopolar and anterior frontal veins are all oriented forward usually with a decreasing angle going from the frontal to the occipital veins. The anatomical descriptions are adopted from Oka et al. (1985). According to this data the eleven largest veins were included by connecting a node on the cortical surface of the brain to a node on the superior sagittal sinus. The resulting length of the bridging vein elements were: Frontopolar—16.5 mm; Anterior Frontal—15.8 mm; Middle Frontal—9.7 mm; Posterior Frontal—13.7 mm; Vein of Trollard—18.4 mm; Precentral—18.2 mm; Central—14.9 mm; Postcentral—15.0 mm; Anterior Parietal—8.8 mm; Posterior Parietal—19.9 mm; Occipital—17.8 mm. A uniform tensile stiffness of 1.9 N per unit strain (Table 1) based on the data from Lee and Haut (1989) was assumed for all bridging veins.

Material Properties

To cope with the large elastic deformations, a Mooney-Rivlin hyperelastic constitutive law was utilized for the CNS tissues. Hyperelasticity is path-independent and fully reversible, and the stress is derived from a strain energy potential. The stored strain energy for a hyperelastic material which is isotropic with respect to the ini-

tial, unstressed configuration can be written as a function of the principal invariants (I_1, I_2, I_3) of the right Cauchy-Green deformation tensor, i.e., $W = W(I_1,I_2,I_3)$. Mooney and Rivlin showed that the simple form

$$W(I_1,I_2) = C_{10}(I_1 - 3) + C_{01}(I_2 - 3) \quad (1)$$

closely matches results from large deformation experiments on incompressible rubber. To model the brain tissue as an unconstrained material a hydrostatic work term, $W_H(J)$, is included in the strain energy functional which is a function of the relative volume, J (Ogden, 1984):

$$W(J_1,J_2,J) = C_{10}(J_1 - 3) + C_{01}(J_2 - 3) + W_H(J) \quad (2)$$

$$J_1 = I_1 J^{-1/3}$$

$$J_2 = I_2 J^{-2/3}$$

In addition, rate effects are taken into account through linear viscoelasticity by a convolution integral of the form:

$$S_{ij} = \int_0^t G_{ijkl}(t - \tau)\frac{\partial E_{ij}}{\partial \tau} d\tau \quad (3)$$

in terms of the second Piola-Kirchhoff stress, Sij, and Green's strain tensor, Eij. This stress is added to the stress tensor determined from the strain energy functional. The stress relaxation function, Gijkl, is represented by two terms in a prony series, given by:

$$g(t) = \sum_{i=1}^{N} G_i e^{-\beta_i t} \quad (4)$$

This is effectively a Maxwell fluid that consists of dampers and springs in series, where G_i are the shear moduli, and β_i are the decay constants. Mendis et al. (1995) derived the rate dependent Mooney-Rivlin constants C_{10} and C_{01} and time decay constants β_i, using experiments published by Estes and McElhaney (1970) on white matter from the region of the corona radiata.

Using the relationship $G = 2(C_{10} + C_{01})$ for the prony terms gives the following constants: $G_1 = 8149$ Pa, $\beta_1 = 125$ 1/sec, $G_2 = 4657$ Pa, and $\beta_2 = 6.67$ 1/sec. The law has been introduced for both white matter (Estes and McElhaney, 1970) and the gray matter (Prange et al., 2000). The Mooney-Rivlin constants for the brain stem were assumed to be 80% higher than those for the gray matter in the cortex (Arbogast and Margulies, 1997). For the spinal cord and cerebellum, the same properties as for the white and gray matter were assumed due to lack of published data.

Although significantly less stiff than those used in previous 3D FE models of the human head, these parameters give a stiffness for the brain tissue that is higher than the average published values (Donnelly, 1998). Two additional, more compliant models were therefore implemented. The stiffness parameters C_{10}, C_{01}, G_1, and G_2 were scaled down while the decay constants were not altered. One model used properties corresponding to an instantaneous shear modulus of around 750 Pa, which is slightly less than the most compliant data available on brain tissue (Prange et al., 2000). In an intermediate model, the properties were adjusted to levels near the average values reviewed by Donnelly (1998), giving an instantaneous shear modulus of around 1.5 kPa. A summary of the properties for the other tissues of the human head used in this study is shown in Table 1.

Interface Conditions

The dura is often adhered to the skull, thus the interface between the skull and the dura was modeled with a tied contact definition in LS-DYNA (Livermore Software Technology Corporation, 2001). Because of the presence of CSF between the meningeal membranes and the brain, sliding contact definitions were used for these interfaces. The chosen contact definition allowed sliding in the tangential direction and transfer of tension and compression in the radial direction. This was done in part because a fluid structure interface is likely to experience a vacuum when a pressure wave reflects at the contrecoup site, or when inertial forces create tension in brain regions opposite to the impact. An average CSF thickness of roughly 2 mm was used, which corresponds to approximately 120 mL of subdural and subarachnoid CSF. A coefficient of friction of 0.2 was used, as proposed by Miller et al., (1998). The subdural and subarachnoid CSF, as well as the ventricular CSF, was modeled with eight node brick elements and a fluid element formulation. The outer boundary of the elements representing the ventricles was joined to the brain tissue elements through common nodes.

Head Injury Criterion and Head Impact Power

The HIC and the HIP, were calculated according to the formulas below.

$$HIC = \left[\frac{1}{(t_2 - t_1)}\int_{t_1}^{t_2} a(t)dt\right]^{2.5}(t_2 - t_1) \quad (5)$$

$$HIP = ma_x\int a_x dt + ma_y\int a_y dt + ma_z\int a_z dt + I_{xx}\alpha_x\int \alpha_x dt + I_{yy}\alpha_y\int \alpha_y dt + I_{zz}\alpha_z\int \alpha_z dt \quad (6)$$

The *x*-axis was defined along the PA direction, the *y*-axis along the lateral-direction, and the *z*-axis in the Inferior-Superior (IS) direction. The following values were calculated for the model: $m = 4.37$ kg, $I_{xx} = 0.0213$ kgm^2, $I_{yy} = 0.0275$ kgm^2, $I_{zz} = 0.0204$ kgm^2. These values are

Table 1. Properties Used in the Numerical Study

Tissue	*Young's modulus [MPa]*	*Density [kg/dm^3]*	*Poisson's ratio*
Outer table/face	15,000	2.00	0.22
Inner table	15,000	2.00	0.22
Diploe	1000	1.30	0.24
Neck bone	1000	1.30	0.24
Neck muscles	0.1	1.13	0.45
Brain	Hyperelastic/viscoelastic	1.04	0.4999994
Cerebrospinal fluid	K = 2.1 GPa	1.00	0.5
Sinuses	K = 2.1 GPa	1.00	0.5
Dura mater	31.5	1.13	0.45
Falx/tentorium	31.5	1.13	0.45
Scalp	16.7	1.13	0.42
Bridging veins	EA = 1.9 N		

K, bulk modulus; EA, force/unit strain.

in the range of reported ones by Becker (1972) and Walker et al. (1973).

Scaling of the Power Index to Account for Directional Sensitivity

In addition, a modified HIP, called the Power Index (PI) with scaling coefficients for the various directions and differentiation between positive and negative accelerations, were calculated using the formula:

$$PI = [C_1^+\theta(a_x) + C_1^-\theta(-a_x)]ma_x\int a_x dt + C_2 ma_y\int a_y dt + [C_3^+\theta(a_z) + C_3^-\theta(-a_z)]ma_z\int a_z dt_x + C_4 I_{xx}\alpha_x\int \alpha_x dt + [C_5^+\theta(\alpha_y) + [C_5^-\theta(-\alpha_y)]I_{yy}\alpha_y \int a_y dt + C_6 I_{zz}\alpha_z\int \alpha_z dt \quad (7)$$

where θ(a) is the Heaviside's step function defined by:

$$\theta(a) = \begin{cases} 1, a > 0 \\ 0, a < 0 \end{cases}$$

This formula is a modified version of the original PI (Newman et al., 2000), proposing a way of taking into account consequences of opposite directions using the Heaviside's step function.

A total of nine acceleration pulses (pure translation and angular) were applied to the center of gravity of the head in the ± PA, ± SI, and in the lateral directions (Fig. 2), in order to look into directional differences and to derive the scaling factors in Eq. 7. In the study of the angular acceleration components, a squared sinusoidal pulse

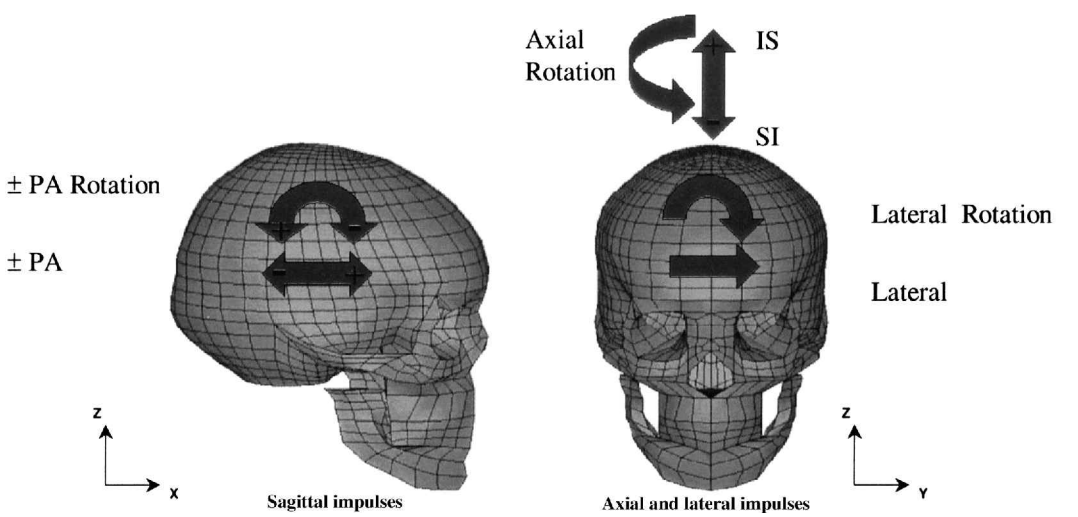

FIG. 2. Load directions for translational and angular acceleration pulses.

(sin^2) with an amplitude of 20–23.2 krad/sec^2 and a duration of 5 msec, was used, resulting in a peak angular velocity of 50–58 rad/sec (in the range of the proposed threshold for DAI by Margulies and Thibault, 1992), and a HIP_{max} of 17.3 kW for all directions. To obtain a comparison with the angular impulses, a squared sinusoidal pulse with an amplitude of 1580 m/sec^2 and a duration of 5 msec was used for the translational impulses resulting in a HIC of 295 and a HIP_{max} of 17.3 kW.

Since the head is assumed to be symmetric around the sagittal plane, only the coefficients for the sagittal and axial directions of the PI have distinct values for ± directions. To make a comparison with the concussion data and HIP values presented by Newman et al. (2000), the lateral translational acceleration impulse was used as a basis for the scaling coefficients of the other directions. This was done since the NFL concussion data, used in that study were predominantly lateral and translational. Head injury is assumed to correlate with the maximum value of HIP and PI achieved by Eqs. 6 and 7 during an impact, named HIP_{max} and PI_{max}, respectively. The scaling constants for the prediction of SDH (PI_{SDH}) were based on the strain in the individual bridging veins. The maximal value of the strain in the bridging veins during a simulation was used to derive the scaling constants for the PI_{SDH}.

Evaluation of the Power Index

To evaluate the ability of the PI to predict injury, four mixed loading plane simulations were performed. The head models were impacted frontally, temporally, and occipitally with a velocity of 5 m/sec towards a padded surface to simulate more realistic accident scenarios (Fig. 3). The padding was inclined 45o in the sagittal direction, as well as rotated 45° in the axial direction to induce angular acceleration pulses, in addition to the translational ones. The padding was 25 mm thick, and modeled as a foam material.

The models were used to investigate the differences in terms of maximal engineering strain in the bridging veins, ϵ, and the maximal relative motion between the brain and the skull, due to variation in impact direction. Furthermore, the HIC, the HIP and the PI were evaluated, with respect to the strain in the bridging veins in an effort to predict consequences of different impact directions.

Experimental Validation

Results from simulations with the FE model were compared with the relative displacement recordings from experiments presented by Al-Bsharat et al. (1999) (Fig. 4). The cadaver head experiments focused on measuring the relative skull-brain motion using high-speed biplanar x-ray system and neutral density targets (NDT). The NDTs were implanted in two vertical columns located in the occipito-parietal region, and in the tempoparietal region, with a space between the centers of the NDTs of approximately 10 mm. The inverted cadaver head was suspended in a fixture that allowed rotation and translation. Occipital impacts were conducted on the specimen (Fig. 4, upper left). The rigid body motion of the skull were eliminated from the NDT (brain) motion data, leaving the skull–brain relative displacement magnitude.

RESULTS

When comparison was made between earlier experiments and the present FE model, a significant correlation in skull-brain relative displacement magnitude could be seen (Fig. 4). The results of three locations in the occipito-parietal region for a 3.6 m/sec impact is seen in Figure 4, and are used as a measure of the FE models abil-

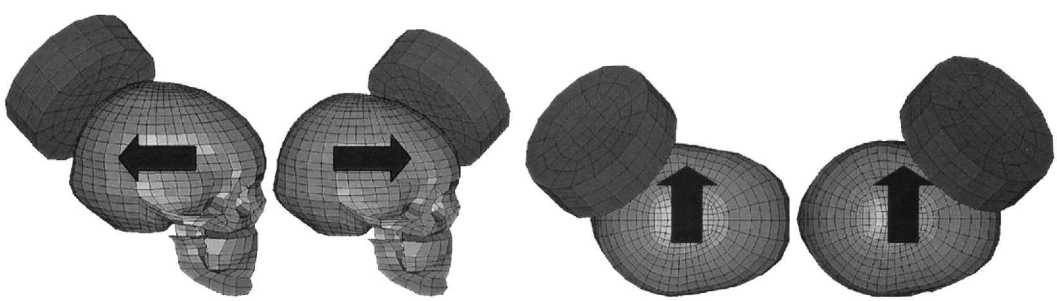

FIG. 3. Impact directions.

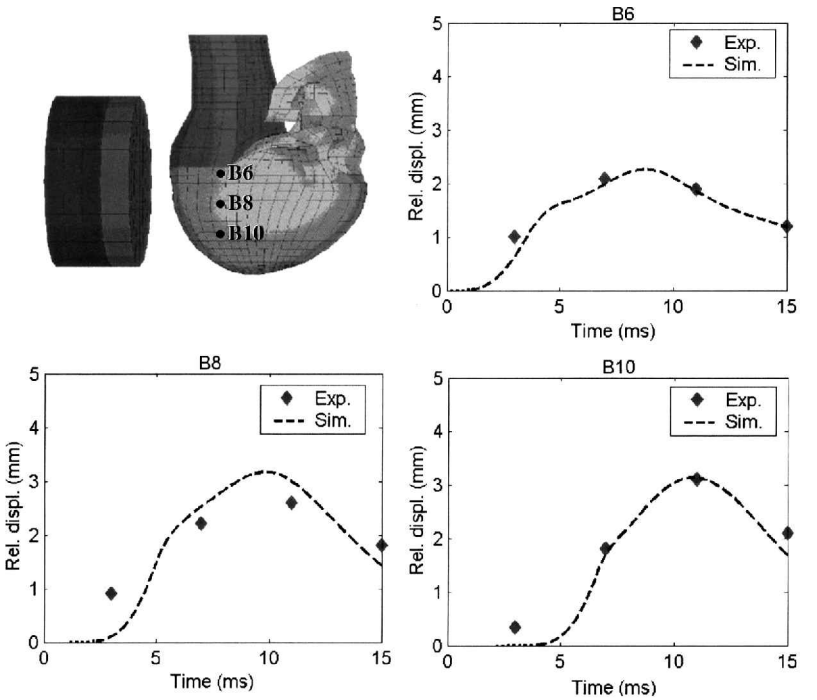

FIG. 4. Experimental comparison of relative motion between the brain and skull.

ity to describe relative motion between the skull and the brain.

Directional Sensitivity

A summary of the results from the comparison of translational and angular impulses in different directions is shown in Table 2. It can be seen that the largest skull–brain relative motion and strain in the bridging veins appears for the AP and PA rotational impulses, while a small relative motion and a zero strain in the bridging veins is recorded for the SI translational impulse (Table 2). This supports the hypothesis of varying responses in relative motion between the skull and the brain and strain in the bridging veins for a change in the impact direction to the human head.

For the angular impulses, the same HIP_{max} values are calculated as for the translational impulses, while the HIC is equal to zero for a pure rotational impulse. Nevertheless, larger relative motion between the skull and the brain as well as higher strain in the bridging veins occur with the rotational impulses. For this type of loading, the worst case is the PA rotation where the highest strain in the bridging veins appears. Almost a threefold increase

TABLE 2. RESULTS FOR DIFFERENT DIRECTIONS AND TRANSLATIONAL AND ANGULAR ACCELERATION IMPULSES

Direction	*Relative motion (mm)*	*Area of max rel. motion*	*Strain in bridg. vein (%)*	*Location of max strain*
AP	1.2	Precentral	4.4	Anterior frontal
PA	1.1	Precentral	8.9	Anterior parietal
SI	0.7	Posterior parietal	0.0	
IS	0.9	Posterior parietal	4.9	Anterior parietal
Lat.	0.7	Middle frontal	7.1	Middle frontal
AP rot.	3.1	Vein of Trollard	11.1	Anterior frontal
PA rot.	3.1	Precentral	33.3	Anterior parietal
Axial rot.	0.9	Middle frontal	9.7	Middle frontal
Lat. rot.	1.2	Posterior frontal	8.9	Middle frontal

AP, anterior-posterior; PA, posterior-anterior; SI, superior-inferior; IS, inferior-superior; Lat., lateral; Rot., rotation.
HIP_{max} = 17.3 kW, HIC = 0 for the angular impulses, while HIP_{max} = 17.3 kW and HIC = 295 for the translational impulses.

in the relative skull-brain motion is found for the PA and AP impulses, when switching from a translational to a rotational mode of motion. Similar results are found for the strain in the bridging veins, but more pronounced for the PA direction. In this case, an increase of almost four times is found when changing to rotational motion. For the lateral direction, a smaller sensitivity to the mode of motion is found. Only a 71% increase in relative motion and a 25% increase in the strain of the bridging veins are observed when changing from a lateral translational to a lateral rotational motion.

The maximal strain occurred in the bridging veins which are directed in the plane of the motion and are angled in the direction of motion. This is obvious for the PA impulses simulating an occipital impact where the PA oriented anterior parietal veins endured the largest strain. The same holds true for the lateral direction where the laterally oriented middle frontal veins sustained the largest strain.

Also, the strain in the bridging veins and the relative motion at the skull-brain interface show a small sensitivity to the shear properties utilized for the brain tissue. A 6.9% increase in the strain in the bridging veins were found for the stiffest properties when compared to the results from the most compliant model for the PA rotational impulse. Since the most compliant properties (Prange et al., 2000) correspond to an instantaneous modulus that is around 20 times more compliant than the stiffest properties used in this study (Mendis et al., 1995), this difference must be considered as insignificant.

The maximal effective stresses and shear strains in the brain occurred at a later time (6.0–10.0 msec) than the maximal strain in the bridging veins (3.0–4.5 msec). This time lag of the strain observed in the bridging veins were more pronounced for the rotational degrees of freedom.

Images showing a top view of the straining of the central and parietal bridging veins when enduring the PA rotational impulse simulating an occipital impact can be seen in Figure 5. Note the change in the angle of the central and parietal veins as the brain lags, while the skull and the superior sagittal sinus are accelerated in the PA direction.

Derivation of Scaling Constants

Based on the strain in the bridging veins for the various directions individually (Table 2), the scaling constants for the PI in equation 7 were determined for SDH (PI_{SDH}) (Table 3). The strain in the bridging veins due to a lateral translation ($\varepsilon = 7.1$ %) was used as the basis of the scaling. This was done to make a comparison with the predominantly translational, lateral impact data presented by Newman et al. (2000). This gave $C_2 = 1.00$ for the lateral translational direction.

Evaluation of the Power Index

The head acceleration characteristics from the FE simulations were used as a basis for the calculations of HIC, HIP, and PI_{SDH}. The accelerations for the lateral impact to the Occiput is shown in Figure 6 below. It can be seen that all the translational accelerations are significant, while mainly the x- and z-angular accelerations contribute to the injury assessment functions for this impact case. The accelerations, and velocities were distinct for the varying impact directions, giving a diverse material for evaluation of the injury criteria.

Considering the frontal, lateral, and occipital impacts towards inclined, rotated and padded surfaces, the largest strain levels in bridging veins were recorded in the middle frontal vein for the occipital impact (Table 4). For

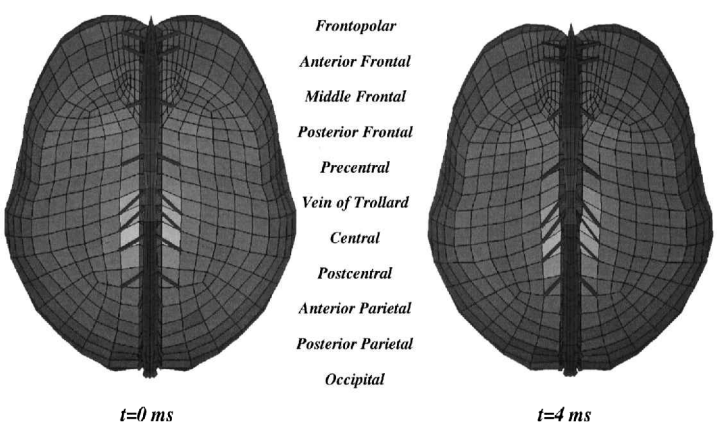

FIG. 5. Straining of the central and parietal bridging veins when enduring the PA rotational impulse, before impact on the left side, and at about 4 msec on the right side (at maximum).

Table 3. Scaling Coefficients for the Power Index (PI) in Equation 7 Based upon the Maximal Strain in the Bridging Veins

	C_1^+	C_1^-	C_2	C_3^+	C_3^-	C_4	C_5^+	C_5^-	C_6
Direction	PA	AP	Lat.	IS	SI	Lat. rot.	AP rot.	PA rot.	Axial rot.
Scaling coefficient	1.25	0.62	1.00	0.69	0.00	1.25	1.56	4.69	1.37

strain in the bridging veins, the impacts toward the occipital area seem to be more severe than the ones to the frontal area, although values for the HIC and HIP are similar for all load directions. Moreover, it can be seen that using the proposed scaling procedure, an improved prediction of the risk of SDH due to failure of the bridging veins can be obtained. This is seen for the occipital impact where both the highest strain in the bridging veins and the largest PI_{SDH} are found. Correspondingly, the smallest strain in the bridging veins and the largest PI_{SDH} are found for the frontal impact. However, the lateral impact to the front and the lateral impact to the occiput resulted in intermediate strain levels in the bridging veins which did not correspond to the predicted PI_{SDH}.

Comparison with Tissue Thresholds

Applying an increasing HIP by augmenting the angular acceleration magnitude while keeping the duration of the squared sinusoidal impulse constant gave an elevation of the relative skull-brain displacement as well as the strain of the bridging veins for the PA rotational direction (Fig. 7). Also, for this direction, a risk of SDH is found for a HIP of around 50 kW. This is clear since a strain of the anterior parietal vein close to the reported failure strain of 50 percent (Lee and Haut, 1989) is observed (Fig. 7, left).

DISCUSSION

The present results verify the hypothesis that a variation in load direction alters the outcome of an impact to the human head. Based on this FE model, new global head injury criteria can be evaluated for all the degrees of freedom of the head. Here, the injury criteria are valid for a larger range of impact conditions. Injury criteria are

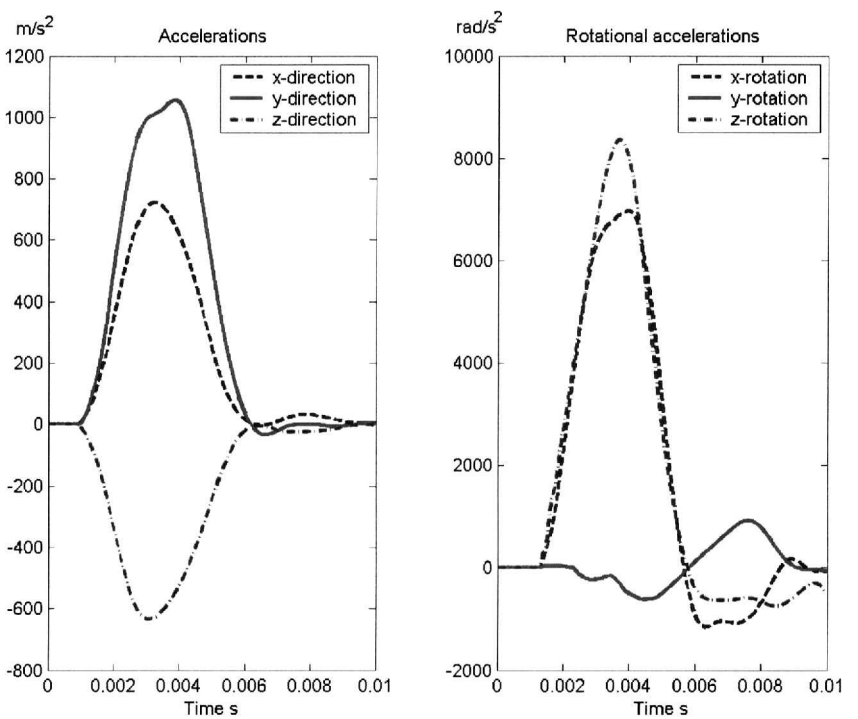

FIG. 6. Head accelerations (at the c.g.) from the FE simulation of a lateral impact to the occiput.

TABLE 4. RESULTS FOR DIFFERENT IMPACT DIRECTIONS TOWARDS PADDED SURFACES

Direction	*Strain in bridg. vein (%)*	*Location of max. strain*	*HIC*	*HIP (kW)*	PI_{SDH} *(kW)*
Front. imp.	1.6	Anterior frontal	362.6	24.8	13.4
Occ. imp.	9.5	Middle frontal	378.8	25.1	32.6
Lat. imp. fr.	4.9	Middle frontal	284.3	26.4	25.3
Lat. imp. occ.	7.0	Middle frontal	318.8	24.7	24.4

today based on a few load directions, but in real life and as indicated by this study, the outcome for different intracranial components varies depending on the load direction.

The analysis showed that the maximal strain occurred in the shortest bridging veins which are oriented in the plane of the motion and are angled in the direction of motion. This might be explained by the anatomical differences in length and orientation between the bridging veins. This is evident for the PA impulses simulating an occipital impact, where the largest skull-brain relative displacement is found around the longer, laterally oriented precentral veins, while the shorter, anterior parietal veins which are directed forward endured the largest strain. This is also seen for the lateral translational direction, where the shorter and laterally oriented middle frontal veins endured the largest strain although the largest skull-brain relative displacement is found around the longer posterior frontal veins. When enduring a lateral impact, the lower values of strain in the bridging veins compared to the occipital impacts could probably be explained by the supportive properties of the falx cerebri. The present study supports the findings of Gennarelli et al. (1982, 1987). This is evident since smaller relative motion between the brain and skull for a lateral impulse compared to a corresponding sagittal one suggests the influence of the falx cerebri, which may impinge upon adjacent structures such as the corpus callosum, potentially causing injury. This is also supported by the findings of higher principal strains in the corpus callosum for a coronal rotation compared to a sagittal rotation when delivering a acceleration pulses corresponding to the same head impact power (HIP) which has been reported previously (Kleiven and von Holst, 2002c). The supportive nature of the falx can also explain the smaller increase in the relative displacement between the skull and the brain when changing from a translational lateral motion to a corresponding rotational motion.

The importance of impact directions in causing SDH is also supported by previous studies. Hirakawa et al. (1972) studied 309 adult cases of chronic SDH, and found that sagittal blows were the dominant cause. They also found that nine out of 27 cases of SDH due to sport accidents were caused by judo when people "fell down on their back."

Fruin et al. (1984) found that six out of eight cases of interhemispheric SDH with known trauma sites were due to occipital impacts. This supports an earlier study by

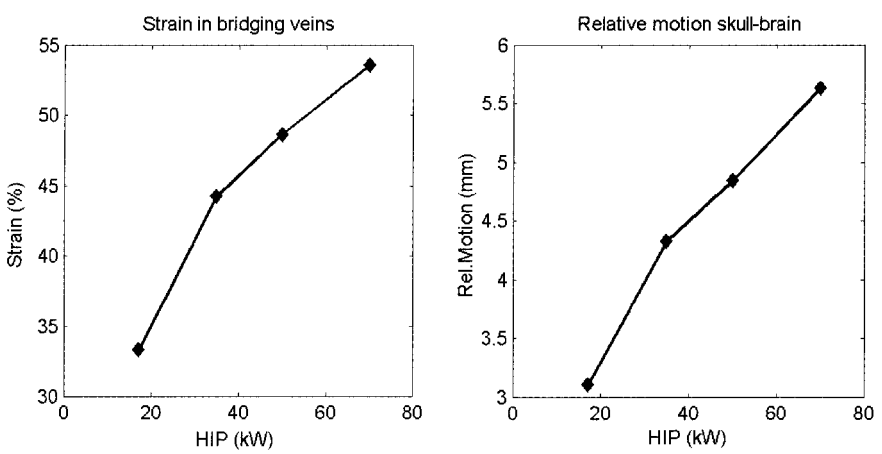

FIG. 7. The maximal strain in the bridging veins (left) and the maximal relative displacement between the skull and the brain (right) as a function of the HIP for the PA rotational impulse.

Jamieson and Yelland (1972), who found that axial (frontal, occipital, or vertical according to their definition) trauma sites accounted for more than half of the simple subdural hematomas. The complicated hematomas were, on the other hand, slightly over represented by lateral trauma sites. Furthermore, the clinical studies by Hirakawa et al. (1972) and Jamieson and Yelland (1972) both reported that SDH were found uncommonly in the occipital region, which supports the results that the largest strains were found for the parietally, centrally or frontally located bridging veins for all impact directions. Gennarelli et al. (1972) subjected 25 squirrel monkeys to controlled sagittal plane head motions, and found brain lesions in both translated and rotated groups but with greater frequency and severity after rotation.

When it comes to relative motion and strains in the bridging veins, the HIP criterion should give a better prediction of the risk of SDH than HIC. This is evident since the HIP takes into account the load direction and the rotational components of the acceleration. However, the only factors that differentiate between directions in the original HIP are the variation in the mass moment of inertia. Newman et al. (2000) therefore proposed a scaling of the impact power for different directions, depending on the tolerance level for the actual direction. The HIP criterion predicts the same levels for the translational impulses as for a corresponding angular impulse, where the highest levels of stresses/strains in the corpus callosum and bridging veins are to be found. This gives an indication that weight factors should be introduced to the components of the HIP criterion in order to predict the consequences of impacts where the angular acceleration components are not negligible and a prediction of SDH is desired.

When comparing the various directions, it can be seen in the case of the translational impulses that different strains in the bridging veins appear when changing the direction from positive to negative as for the AP and PA directions. Thus, the original version of HIP does not distinguish between opposite load direction. In our opinion, three additional components should be added to the original HIP in order to fully take into account the differences in response between opposite directions. This is added using the Heaviside's step function for the sagittal translations and angular motion, as well as for the axial translational motion, as proposed in Eq. 7.

Another problem with HIC and HIP is that they do not seem to capture the level of intracranial response for different impulses. A zero HIC value is predicted for a pure rotational impulse while higher levels of stresses and strains are found compared to a corresponding translational impulse in the same direction. This underlines findings by previous investigators (Gennarelli et al., 1972).

When imposing the scaling coefficients to the PI for the different directions in the prediction of SDH (PI_{SDH}), and when comparing with HIC and HIP, a better correlation between intracranial response and PI-value was found. Using the proposed PI_{SDH}, a substantially lower risk of SDH is predicted for the frontal impact compared to the other directions. This is also the case when looking at the maximal strain in the bridging veins, where insignificant strain is experienced for this impact. However, PI_{SDH} fail to predict the intermediate levels of strain in the bridging veins for the lateral impacts. This is possibly explained by the maximal strain occurring in a different bridging vein for a combined loading than for the single degree of freedom loading cases from which the scaling factors are derived. Moreover, the differences in the intracranial responses for those two cases are quite small, which makes a distinction difficult for a global kinematic based injury assessment function. Another explanation are the as yet unexplored synergic effects of combined loadings. This is included naturally by the product of inertia terms for the angular components in the impact power formulation when using anatomical coordinates. Since the anatomical directions do not coincide with the principal directions of inertia, the product of inertia, I_{xz}, is non-zero. This would add two terms ($I_{xz}a_z \int a_x dt$ and $I_{xz}a_x \int a_z dt$) in equations 6 and 7. In the case of the human head, the power terms containing the products of inertia I_{xy}, I_{xz} and I_{yz} are insignificant compared to the moments of inertia I_{xx}, I_{yy}, and I_{zz} (Becker, 1972; Walker et al., 1973). Nevertheless, these terms in the PI could be estimated using the FE model. In this way, separate scaling factors could be derived to account for synergism of combined directions. In the same manner, supplementary components for the translational terms could also be added to improve the injury prediction.

The maximal effective stresses and principal strains in the brain occurred at a later time than the maximal strain in the bridging veins. This is supported by Gennarelli (1983), who suggested that SDH was produced by short duration high amplitude in angular accelerations, while DAI was produced by longer duration, low amplitude in coronal accelerations.

Evaluation of the required HIP for a specific direction until a certain tissue level is achieved ($\varepsilon = 0.5$ for the bridging veins as proposed by Lee and Haut, 1989) was also estimated using the FE model. A threshold for SDH of around 50 kW for the PI_{SDH} was found for the PA rotational direction, which gave the largest strain in the bridging veins. This corresponds to a rotational acceleration threshold of around 34 krad/sec^2 for a 5 msec duration, resulting in a change in angular velocity of 85 rad/sec. Using collision tests with cadavers Löwenhielm (1974a) found that bridging vein disruption due to rota-

tional movement of the head is obtained when the angular acceleration exceeds 4.5 krad/sec^2 and/or the change in angular velocity exceeds 50 rad/sec. Assuming a squared sinusoidal shape of the angular acceleration impulse for the proposed thresholds of 4.5 krad/sec^2 in angular acceleration and a change in angular velocity of 50 rad/sec would give a HIP of 3.5 kW. The estimation of the rotational accelerations/velocities was based on the planar motion of the head in the sagittal plane excluding any effects of other rotations/translations. In addition, the motions were not purely rotational, and either none or, several bridging veins were ruptured indicating that a real threshold was not found. Also, in these experiments which were previously presented by Voigt and Lange (1971), there was a high level of violence other than the rotational. The non-belted cadavers were seated on a sled and accelerated to velocities of 43–60 km/h before braking to a standstill and impacting against the instrument panels. In some of these experiments, the translational acceleration on the top of the head was recorded. In the more severe cases, translational accelerations varying between $\pm$200 g were recorded, possibly adding substantially to the rotational violence. The threshold of 50 kW for PISDH in the PA rotation compares well with data from Newman et al. (2000), who estimated a 50 % probability of concussion for a HIP of 12.8 kW.

The bridging veins have been reported to have an ultimate strain of about 0.5 in tension (Lee and Haut, 1989); while L^wenhielm (1974b) reported failure strain values ranging from 0.2 to about 1.0 depending on the strain rate. Using the average ultimate strain reported by Lee and Haut (1989), none of the impact directions indicated a risk of SDH. Nevertheless, as in the properties of most biological tissues, there is a great variation among those results. Using the standard deviation reported by Lee and Haut (1989) or the lowest value from Löwenhielm (1974b) suggests a threshold of around 0.2 in the worst scenario. This emphasizes the difference between a pure rotational load and a pure translational load, indicating a substantially lower tolerance for SDH for the rotational impulses, which is not predicted by existing head injury criteria.

The technique of modeling the bridging veins using truss elements could be discussed. However, since a bridging vein normally fails at a point between the first attachment in the cortical area of the brain and the entry in the superior sagittal sinus, the current approach should be sufficient for this study. The properties of the bridging veins are also compliant, and a further inclusion of the continuation in the inferior direction would probably not affect the deformation pattern of the structure as a whole. The compliant nature of the bridging veins also resulted in the decision not to include rupture, or deletion of the truss elements when a certain failure strain occurs. The 11 parasagittal veins that were included in the model were chosen based on their size; only the largest veins were included. The fact that no data for the average angle towards the superior sagittal sinus were available for the smaller veins also contributed to this choice.

Because motion between the brain and skull during head impact has been considered potentially important to head injury for more than 50 years (Pudenz and Shelden, 1946; Gurdjian et al., 1968), a primary concern in FE modeling of the human head has been the interface between the brain and skull. Fluid elements should be used to simulate the CSF as proposed by Zhou et al. (1995), Bandak and Eppinger (1994), Miller et al. (1998), and Al-Bsharat et al. (1999) in order to adequately represent the effect of the ventricles and the skull–brain interface. However, adequate representation of fluid-structure interaction still remains a major limitation of most commercially available FE packages. Due to this problem, two different approaches that do not implement fluid elements for the CSF have been developed to model the skull-brain interface. The first approach models the subarachnoid CSF using linear elastic solid elements with low shear modulus. This approximation has been used by several researchers (Ruan et al., 1997; Willinger et al., 1995; Turquier et al., 1996; Zhou et al., 1995). Even with a low shear modulus for the CSF, this method is likely to induce shear stress and strain, and to cause computational instability because of the large element distortions that result from using them in the brain–skull interface. An alternate way of modeling the brain–skull interface includes contact algorithms between the brain and the dura mater. The contact has been defined in different ways ranging from completely fixed to frictionless sliding. Several parametric studies have been performed, where the effects of different interface conditions between brain and skull have been studied (Cheng et al., 1990; Claessens et al., 1997; Bandak and Eppinger, 1994; Miller et al., 1998). All of them conclude that the impact response of the human head is sensitive to the modeling of this interface condition. The sliding (with separation) contact algorithm used by Kuijpers et al. (1995) and Claessens et al. (1997) was found to be insufficient for the brain–membrane interfaces in the contrecoup region, and a gap was created in this region due to limited load transfer to compression only. In our study, a sliding-only contact algorithm, which transfers load in tension was also implemented. Because of this, large relative motion between the brain and skull was allowed and the load was supported in tension at the contrecoup region. This resulted in comparable magnitude of the skull-brain relative displacements between the simulations and experiments.

Comparison of results from the FE model with experimental measurements of relative displacement between the skull and the brain presented by Al-Bsharat et al. (1999) shows a good correlation reaching the magnitudes of the relative displacements in the experiments. When it comes to the characteristics, it is difficult to draw any conclusions because the experiments were conducted with a sampling rate of 4 ms. Due to the fact that the experimental impacts are mostly translational, it is also reasonable to believe that the intracranial contents should respond in the same manner, i.e. with little relative skull-brain motion. A comprehensive correlation between the FE model output and relative motion between the human cadaver brain and skull in anatomical X, Y, and Z components (Hardy et al., 2001; King et al., 2002) for higher magnitude rotational loading conditions has previously been demonstrated by Kleiven and Hardy (2002).

Despite some limitations of an FE approach, the results of this study should be taken into consideration when developing safety systems in general. It can also be shown that the intracranial responses vary in a different manner for the various intracranial components when changing impact directions (Kleiven and von Holst, 2002c). Thus the PI should be a unique function, depending on the injury mechanism to be studied.

CONCLUSION

It is stressed that the scaling procedures and coefficients are proposed estimations using a parameterized and detailed FE model of the human head. Although the results give insight into directional sensitivity of impacts to the human head, further experimental validation of intracranial responses for the model in response to higher rotational loads needs to be performed before new head injury criteria can be suggested.

Regarding the influence of inertial forces to all the degrees of freedom of the human head, this study shows the following:

1. The results obtained by the FEM correlate with previous clinical and animal studies.
2. HIC is unable to predict consequences of a pure rotational impulse while HIP needs individual scaling coefficients for the different terms to account for difference in load direction.
3. Three additional components, implemented as Heaviside's step functions, should be added to the original HIP in order to take into account the differences in response between opposite directions.
4. When using the proposed scaling procedure, a better prediction of SDH was obtained.
5. Further evaluation of synergic effects of combined terms of the PI is necessary to improve the injury prediction.

ACKNOWLEDGMENTS

This work was supported by the Swedish Transport and Communications Research Board, no. 1999-0847. I wish to thank Prof. Hans von Holst of the Karolinska Institute, Stockholm, for his valuable assistance.

REFERENCES

AL-BSHARAT, A.S., HARDY, W.N., YANG, K.H., et al. (1999) "Brain/skull relative displacement magnitude due to blunt head impact: new experimental data and model, in: *43rd Stapp Car Crash Conf., SAE paper no. 99SC22.* Society of Automotive Engineers, pps. 321–332.

ARBOGAST, K.B., and MARGULIES, S.S. (1997). Regional differences in mechanical properties of the porcine central nervous system, SAE paper no. 973336, in: *41st Stapp Car Crash Conf.* Society of Automotive Engineers, pps. 293–300.

ARBOGAST, K.B., PRANGE, M.T., MEANEY, D.F., et al. (1997). Properties of cerebral gray and white matter undergoing large deformation, in: *Prevention Through Biomechanics, Symposium Proceedings.* Wayne State University, pps. 33–39.

BANDAK, F.A., and EPPINGER, R.H. (1994). A three-dimensional FE analysis of the human brain under combined rotational and translational accelerations, in: *38th Stapp Car Crash Conf.* Society of Automotive Engineers, pps. 145–163.

BAIN, B.C., and MEANEY, D.F. (2000). Tissue-level thresholds for axonal damage in an experimental model of central nervous system white matter injury. J. Biomech. Eng. **16,** 615–622.

BECKER, E.B. (1972). Measurement of mass distribution parameters of anatomical segments, in: *16th Stapp Car Crash Conference, SAE techn. paper no. 720964.* pps. 160–185.

BLATTER, D., BIGLER, E.D., GALE, S.D., et al. (1995). Quantitative volumetric analysis of brain MR: normative database spanning 5 decades of life. Am. J. Neurorad. **16,** 241–251.

CHENG, L.Y., RIFAI, S., KHATUNA, T., et al. (1990). Finite element analysis of diffuse axonal injury, in: *Vehicle Crashworthiness and Occupant Protection in Frontal Collisions, SAE paper no. 900547.* Society of Automotive Engineers.

CLAESSENS, M., SAUREN, F., and WISMANS, J. (1997). Modeling of the human head under impact conditions: a parametric study, in: *41st Stapp Car Crash Conf, SAE paper no. 97338.* Society of Automotive Engineers, pps. 315–328.

DONNELLY, B.R., and MEDIGE, J. (1997). Shear properties of human brain tissue. J. Biomech. Eng. **119,** 423–432.

DONNELLY, B.R. (1998). Brain tissue material properties: a comparison of results. *Biomechanical research: Experimental and Computational, Proc. of the 26th Int. Workshop.* pps. 47–57.

DIMASI, F., EPPINGER, R.H., and BANDAK, F.A. (1995). Computational analysis of head impact response under car crash loadings, in: *39th Stapp Car Crash Conf. SAE paper no. 952718.* Society of Automatic Engineers. pps. 425–438.

DIRNHOFER, R., WALZ, F. and SIGRIST, T. (1979). Zur Mechanischen Belastbarkeit des Tentorium Cerebelli, Z. Rechtsmed. **82,** 305–311.

EUROPEAN TRANSPORT SAFETY COUNCIL. (1999). *Reducing the Severity of Road Injuries Through Post Impact Care.*

ESTES, M.S., and McELHANEY, J.H. (1970). Response of brain tissue to compressive loading. ASME paper no. 70-BHF-13.

FRUIN, A.H., JUHL, G.L., and TAYLON, C. (1984). Interhemispheric subdural hematoma. J. Neurosurg. **60,** 1300–1302.

GENNARELLI, T.A., THIBAULT, L.E., and OMMAYA, A.K. (1972). Pathophysiological responses to rotational and translational accelerations of the head, in: *16th Stapp Car Crash Conf.* SAE paper no. 720970. Society of Automotive Engineers, pps. 296–308.

GENNARELLI, T.A., and THIBAULT, L.E. (1982). Biomechanics of acute subdural hematoma. J. Trauma. **22,** 680–686.

GENNARELLI, T.A., THIBAULT, L.E., ADAMS, J.H., et al. (1982). Diffuse axonal injury and traumatic coma in the primate. Ann. Neurol. **12,** 564–574.

GENNARELLI, T.A. (1983). Head injuries in man and experimental animals: clinical aspects. Acta Neurochir. Suppl. **32,** 1–13.

GENNARELLI, T.A., THIBAULT, L.E., TOMEI, G., et al. (1987). Directional dependence of axonal brain injury due to centroidal and non-centroidal acceleration. in: *31st Stapp Car Crash Conf.* SAE paper no. 872197. Society of Automotive Engineers.

GURDJIAN, E.S., HODGSON, V.R., THOMAS, L.M., et al. (1968). Significance of relative movements of scalp, skull, and intracranial contents during impact injury of the head. J. Neurosurg. **29,** 70–72.

HARDY, W.N., FOSTER, C., MASON, M., et al. (2001). Investigation of head injury mechanisms using neutral density technology and high-speed biplanar x-ray, in: *45th Stapp Car Crash Journal.* SAE paper no. 01S-52. Society of Automotive Engineers.

HIRAKAWA, K., HASHIZUME, K., FUCHINOUE, T., et al. (1972). Statistical analysis of chronic subdural hematoma in 309 adult cases. Neurol. Med. Chir. **12,** 71–83.

HODGSON, V.R., THOMAS, L.M., and KHALIL, T.B., et al. (1983). The role of impact location in reversible cerebral concussion. in: *27th Stapp Car Crash Conf.* SAE paper no. 831618. Society of Automotive Engineers, pps. 225–240.

JAMIESON, K.G., and YELLAND, J.D.N. (1972). Surgically treated traumatic subdural hematomas. J. Neurosurg. 37, 137–149.

KING, A.I., HARDY, W.N., MASON, M.J., et al. (2002). Comparison of relative motion between the brain and skull of the human cadaver for rotation in the coronal and sagittal planes, in: *4th World Congress of Biomechanics.* Calgary, Alberta, Canada.

KLEIVEN, S., and VON HOLST, H. (2002a). Consequences of head size following trauma to the human head. J. Biomech. **35,** 153–160.

KLEIVEN, S., and VON HOLST, H. (2002b). Consequences of brain volume following impact in prediction of subdural hematoma evaluated with numerical techniques. *Traffic Injury Prevention.* **3,** 303–310.

KLEIVEN, S., and VON HOLST, H. (2002c). Influence of direction and duration of impact to the human head, in: *4th World Congress of Biomechanics.* Calgary, Alberta, Canada.

KLEIVEN, S., and HARDY, W.N. (2002). Correlation of an FE model of the human head with experiments on localized motion of the brain—consequences for injury prediction, in: *46th Stapp Car Crash Journal.* Society of Automotive Engineers.

LEE, M.C., and HAUT, R.C. (1989). Insensitivity of tensile failure properties of human bridging veins to strain rate: Implications in biomechanics of subdural hematoma. J. Biomech. **22,** 537–542.

LIVERMORE SOFTWARE TECHNOLOGY CORPORATION. (2001). *LS-DYNA Keyword User's Manual.* Version 960.

LÖVENHIELM, P. (1974a). Strain tolerance of the Vv. Cerebri Sup. (bridging veins) calculated from head-on collision tests with cadavers. Z. Rechtsmedizin **75,** 131–144.

LÖVENHIELM, P. (1974b). Dynamic properties of the parasagittal bridging veins. Z. Rechtsmedizin **74,** 55–62.

MARGULIES, S.S., and THIBAULT, L.E. (1992). A proposed tolerance criterion for diffuse axonal injury in man. J. Biomech. **25,** 917–923.

McELHANEY, J.H., ROBERTS, V.L., and HILYARD, J.F., et al. (1976). *Handbook of Human Tolerance.* Japan Automobile Research Institute Inc., Tokyo, p. 143.

MELVIN, J.W., LIGHTHALL, J.W., and UENO, K. (1993). Brain injury biomechanics, in: *Accidental Injury.* A.M. Nahum and J.W. Melvin (eds), Springer-Verlag: New York, pps. 269–290.

MENDIS, K.K., STALNAKER, R.L., and ADVANI, S.H. (1995). A constitutive relationship for large deformation fi-

nite element modeling of brain tissue. J. Biomech. Eng. **117,** 279–285.

MILLER, R.T., MARGULIES, S.S., LEONI, M., et al. (1998). Finite element modeling approaches for predicing injury in an experimental model of severe diffuse axonal injury, in: *42nd Stapp Car Crash Conf. SAE paper no. 983154.* Society of Automotive Engineers, pps. 155–166.

NATIONAL HIGHWAY TRAFFIC SAFETY ADMINISTRATION, (DOT). (1972). *Occupant Crash Protection—Head Injury Criterion S6.2 of MVSS 571.208.* Docket 69-7, Notice 17. NHTSA, Washington, DC.

NEWMAN, J.A., SHEWCHENKO, N., and WELBOURNE, E. (2000). A proposed new biomechanical head injury assessment function—the maximum power index, in: *44th Stapp Car Crash Conf. SAE paper no. 2000-01-SC16.*

OGDEN, R.W. (1984). *Non-Linear Elastic Deformations.* Dover: Mineola, NY.

OKA, K., RHOTON, A.L., BARRY, M., et al. (1985). Microsurgical anatomy of the superficial veins of the cerebrum. Neurosurgery **17,** 711–748.

PRANGE, M.T., MEANEY, D.F., and MARGULIES, S.S. (2000). Defining brain mechanical properties: effects of region, direction, and species. in: *44th Stapp Car Crash Conf. SAE paper no. 2000-01-SC15.* Society of Automotive Engineers.

PUDENZ, R.H., and SHELDEN, C.H. (1946). The lucite calvarium—a method for direct observation of the brain. II. Cranial trauma and brain movement. *J. Neurosurg.* **3,** 487–505.

RUAN, J.S., KHALIL, T.B., and KING, A.I. (1997). Impact head injury analysis using an explicit finite element human head model. J. Traffic Med. **25,** 33–40.

TURQUIER, F., KANG, H.S., TROSSEILLE, X., et al. (1996). Validation study of a 3D finite element head model against experimental data, in: *40th Stapp Car Crash Conf. SAE paper no. 962431.* Society of Automotive Engineers, pps. 283–294.

UENO, K., and MELVIN, J.W. (1995). Finite element model study of head impact based on hybrid III head acceleration: the effects of rotational and translational acceleration. *J. Biomech. Eng.* **117,** 319–328.

VOIGT, G.E., and LANGE, W. (1971). Simulation of head-on collision with unrestrained front seat passengers and different instrument panels, in: *15th Stapp Car Crash Conference. SAE technical paper no. 710863.* pps. 466–488.

U.S. NATIONAL LIBRARY OF MEDICINE, NATIONAL INSTITUTES OF HEALTH (NIH), DEPARTMENT OF HEALTH & HUMAN SERVICES. (2003). Visible human database. Available: www.nlm.nih.gov/research/visible/visible_human.html.

WALKER, L.B., HARRIS, E.H., PONTIUS, U.R. (1973). Mass, volume, center of mass, and mass moment of inertia of head and head and neck of human body, in: *17th Stapp Car Crash Conference. SAE technical paper no. 730985.* pps. 525–537.

WILLINGER, R., TALED, L., and PRADORE, P. (1995). From the finite element model to the physical model, in: *IRCOBI Conf.* Brunnen, 245–260.

ZHANG, L., YANG, K.H., and KING, A.I. (2001). Comparison of brain responses between frontal and lateral impacts by finite element modeling. J. Neurotrauma **18,** 21–30.

ZHOU, C., KHALIL, T.B., and KING, A.I. (1995). A new model comparing impact responses of the homogeneous and inhomogeneous human brain, in: *Proc. of the 39th Stapp Car Crash Conf. SAE technical paper no. 952714.* Society of Automotive Engineers, pps. 121–137.

ZHOU, C., KHALIL, T.B., and KING, A.I. (1996). Visoelastic response of the human brain to sagittal and lateral rotational acceleration by finite element analysis, in: *Proc. of the 1996 IRCOBI Conf. technical paper no. 1996-13-0003.* Dublin, Ireland.

Address reprint requests to:
Svein Kleiven, Ph.D.
Department of Aeronautics
Royal Institute of Technology
Teknikringen 8
Stockholm SE-100 44, Sweden

E-mail: sveink@kth.se